Chaos, Solitons and Fractals 155 (2022) 111784

Contents lists available at ScienceDirect

Chaos, Solitons and Fractals

Nonlinear Science, and Nonequilibrium and Complex Phenomena

journal homepage: www.elsevier.com/locate/chaos

Frontiers

Control attenuation and temporary immunity in a cellular automata SEIR epidemic model

Michele Mugnaine[a,*], Enrique C. Gabrick[b], Paulo R. Protachevicz[c], Kelly C. Iarosz[d,e], Silvio L.T. de Souza[f], Alexandre C.L. Almeida[g], Antonio M. Batista[b,h], Iberê L. Caldas[c], José D. Szezech Jr[b,h], Ricardo L. Viana[a]

[a] Department of Physics, Federal University of Paraná, Curitiba, PR, Brazil
[b] Postgraduate Program in Sciences, State University of Ponta Grossa, Ponta Grossa, PR, Brazil
[c] Institute of Physics, University of São Paulo, São Paulo, SP, Brazil
[d] Faculdade de Telêmaco Borba, FATEB, Telêmaco Borba, PR, Brazil
[e] Graduate Program in Chemical Engineering Federal Technological University of Paraná, Ponta Grossa, PR, Brazil
[f] Federal University of São João del-Rei, Campus Centro-Oeste, Divinópolis, MG, Brazil
[g] Statistics, Physics and Mathematics Department, Federal University of São João del-Rei, Ouro Branco, MG, Brazil
[h] Department of Mathematics and Statistics, State University of Ponta Grossa, Ponta Grossa, PR, Brazil

ARTICLE INFO

Article history:
Received 20 August 2021
Revised 22 December 2021
Accepted 30 December 2021
Available online 10 January 2022

Keywords:
Disease spread model
Cellular automaton
Restriction measures
Second wave of infections
Reinfection

ABSTRACT

Mathematical modeling is an important tool to analyze impacts and plan to mitigate epidemics in communities. In order to estimate the impact of control measures in a second wave of infections, we analyze the SEIR epidemic model based on stochastic cellular automata. The control measure is based on one of the key strategies to control the epidemic, which is the restriction of the mobility of individuals in space. For stronger restrictions, we observe a decrease larger than 15% in the total number of infected individuals during the epidemic. On the other hand, the total attenuation of control measures in the system can lead to a second wave scenario and even a situation in which the total number of infected individuals is close to the uncontrolled case. Additionally, we also include the possibility of reinfection, as the SEIRS model, where the recovered individuals can go to the susceptible state based on a fixed immunity time or a probabilistic rule. Our results show that an extinction of the epidemic occurs only for a fixed immunity time.

© 2022 Elsevier Ltd. All rights reserved.

1. Introduction

An epidemic can be defined as an outbreak of a disease capable to infect a significant portion of the population before it ends [1]. The spread of an infectious disease can happen in different ways. There are transmissions by direct contact with infected individuals or by indirect contact, such as through disease vectors agents, for example. Mathematical models can be considered as methods to study the consequences and to estimate the future of the disease spread [2,3]. They are crucial to understand the epidemic evolution and the impacts of mitigation measures applied to the population, for the purpose of lessening the disease severity, *i.e.*, decreasing the number of infected individuals [4–6].

The epidemiological models, from the compartmental approach (as SIR, SEIR, SI and others) to the Richards growth model, are mostly based on ordinary differential equations (ODE) [4,7]. The ODE models give the infected population time evolution. These models do not consider the individual role in the epidemic evolution, such as the movement of these individuals, the contact processes and a different individual susceptibility [4,7,8].

One way to overcome these limitations imposed by the ODE's models is to implement Individual-Based-Modeling (IBM), taking the individual as a basic unity in the system. By this portrait we include individuals particularities and their influences on the disease spread. One example of IBM is the model based on Cellular Automaton (CA). Cellular automata are discrete dynamical systems with discrete time and space, and the associated physical quantities also admit discrete values. As mentioned by Wolfram [9], physical systems with discrete elements and local iterations are often modeled by CA. In this portrait, we can use CA models to describe epidemics by discretizing the space, considering an IBM model in which the discrete unity in the space is represented by the individual, and the discrete unity in time is a time step (hours or a day,

* Corresponding author.
E-mail addresses: mmugnaine@gmail.com, jdsjunior@uepg.br (M. Mugnaine).

https://doi.org/10.1016/j.chaos.2021.111784
0960-0779/© 2022 Elsevier Ltd. All rights reserved.

for example). Cellular automata based models were already used to generic epidemics and specific diseases detailed in the papers [4,6–8,10–17] and references therein.

Various studies consider different properties of the individuals in the CA model, for example, the heterogeneity of the populations, as different susceptibility and infectivity [10] or the sex ratios, age and individual immunity [6]. Some surveys consider the movement of the individual in space [4,6,13,14,16], or the movement of the vector agent responsible for the infection [15].

In addition to the inclusion of individual particularities, different interaction processes can also be considered by CA based models, as the segregation of infected individuals. In order to attenuate the impact of the epidemics of a disease spread by contact in the population, the implementation of mitigation strategies is crucial. Key strategies such as vaccines, isolation, quarantine, travel restrictions, and drug distribution are necessary and very important [18]. If the vaccines and drugs are absent, the non-pharmaceutical and the preventive measures are the only possibility to reduce the impacts of the epidemic. This topic became a central debate since the outbreak of COVID-19 epidemic in December 2019, declared as a pandemic in early March 2020. Several studies analyzed the impacts of the quarantine of infected individuals and developed mathematical models to forecast the future of the COVID-19 spread [6,19–25].

Besides the impact of control measures, it is also important to study the impact of prematurely easing these measures leading to the possibility of subsequent waves of infections [26]. Souza and coauthors showed that, for the SEIR model with an ODE portrait, a relaxation in the mitigation measures leads to a second wave scenario of the infection curve [22]. A second wave scenario was also predicted by Xu, Qi and Hu [26], as well as by Renardy, Eisenberg and Kirschner [27] for a compartmental model with differential equations description.

The second wave scenario has been studied by means of differential equations and they do not take into account the behavior of the individuals and the possibilities of directed measures in the population for the control of the epidemics. With this perspective, we propose a CA model, based on the compartmental SEIR model, to study the control measures and the possibility of a second wave of infection by the relaxation of these measures. We show that stronger restriction can decrease the total number of infected individuals. In order to also study the possibility of the perpetuation of the disease in the population and subsequent waves of infections, we also consider the loss of immunity of the recovered individuals, as the SEIRS model. A loss of immunity can be, for example, a specificity of the disease or can be a consequence of a new strain of the disease-causing agent. Our results show that, for a fixed immunity time, the end of the epidemic is possible.

This study is organized as follows: In Section 2 we present our model based on cellular automata to describe a disease with a latent period (exposed and not infectious individual) and permanent immunity. In this section, we also expose how the control measures are implemented and eased in the system. The results about the infection control and the probability of a second wave scenario are shown in Section 3. Section 4 is centered in the model with the inclusion of reinfection and we study the impact of a single implementation and relaxation of control measures in the system. Our conclusions are stated in Section 5.

2. SEIR Model and the cellular automata

2.1. Mobility and transition rules

The SEIR model is a well established mathematical set composed of four equations which describe the time evolution of four populations embraced by the model. The susceptible (S) population is composed of healthy individuals and they can become sick. The first stage of the disease is the exposed state (E), where the individuals are sick but they are not infectious or the individuals are sick and they can infect other healthy ones, but with low frequency [8,12]. This model has been considered to study diseases with a latency period. After the latency time, the individual is infected (I) and it can infect other people with a high probability. Lastly, we have the recovered population (R), individuals who can not be infected again.

According to the differential equation formulation, the time evolution for each population of the SEIR model is described by [1]:

$$\begin{aligned} \dot{S} &= -\beta SI, \\ \dot{E} &= \beta SI - \kappa E, \\ \dot{I} &= \kappa E - \alpha I, \\ \dot{R} &= \alpha I, \end{aligned} \tag{1}$$

where the parameters β, κ, and α denote the transition rates of individuals from one population to another. According to the review performed by Brauer and Castillo-Chavez, the equations in (1) represent the case where the exposed individuals are not infectious [1].

The SEIR model presented above considers a fixed number of individuals, *i.e.*, the birth and death rates are not considered in the model. In this study, we follow the same method and the total population $N_T = S + I + E + R$ does not change. Some results from the SEIR model with variable N_T can be found in [5,28–33].

Ordinary differential equations (ODE), similar to the ones in (1), form the basis for most mathematical models of disease spread and epidemic simulation [4]. These models are well consolidated and they were extensively studied. However, they present some limitations related to a high computation time to solve the equations [11] and they do not consider microscopic aspects or individuals properties, as the contact process, the effects of mixing patterns of the individuals, the spatial aspects of the epidemic, a possible heterogeneous interaction between individuals, the motion of the individual in the available space and others individual particularities [4,7,10,11,34].

One way to solve these limitations is the utilization of CA to simulate the spreading of the disease [4,7]. As mentioned in the previous section, a CA is a mathematical model where time and space are discrete [9]. In a practical way, the CA is composed of a regular uniform lattice, where each site (cell) is in a state described by a discrete variable and the cell state evolves at each time step following a set of rules based on the states of their neighbors [9,35]. In this way, we can identify and modify the local interactions by specifying the rules followed in the time evolution.

The studies of the SEIR model in a CA context consider, in general, that each site is occupied by a single individual, which can be in the susceptible (S), exposed (E), infected (I) or recovery (R) state. One individual interacts with its neighborhood that can be four (von Neumann) or eight (Moore) closest sites. The neighborhood can even be more complex, as studied by Gang and coauthors [12], and one site can be filled with more than one individual [4,15]. In our simulations, we consider just one individual per site and the von Neumann neighborhood. The infectious process occurs by the contact between susceptible and infected individuals. In the CA, this happens when an individual in a S state has neighbors in I state.

The model that we analyze in this study was proposed by Quan-Xing and Zhen [8] as a SEIRS epidemic spread model by the probabilistic cellular automata perspective. The model considers five populations: susceptible, exposed, infected, recovery and dead, where every individual belongs to one of these five states. The disease progresses in the following order: the susceptible in-

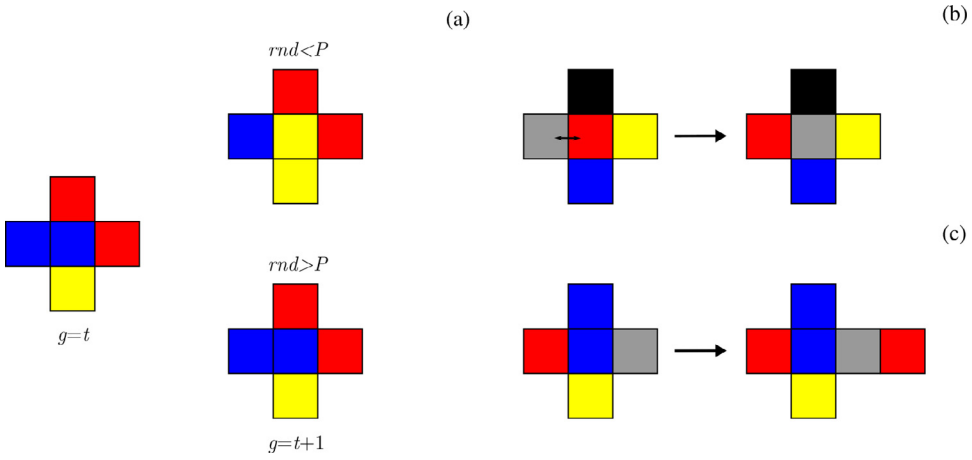

Fig. 1. Illustrations for the (a) transition $S \to E$, (b) mobility in the grid and (c) the neighborhood for the transition $S \to E$ when an empty site is present. In (c), the neighborhood is expanded, where the closest direct neighbor to the empty site, in this schematic figure the red site on the right, is considered for calculating the probability P. In all figures, squares in blue, yellow, red, black and gray represent susceptible, exposed, infected, recovered and empty sites, respectively. (For interpretation of the references to colour in this figure legend, the reader is referred to the web version of this article.)

dividual becomes exposed after contact with infected individuals, after the latency time the individual becomes infected and then it recovers after the infection period, or dies, and the recovered individuals become susceptible again [8].

In the present study, we are interested in the SEIR portrait, in which the recovered individuals stay in this state, *i.e*, the immunity is persistent. The CA is based on a regular lattice $N \times N$, where each site contains only one individual, and the lattice obeys a periodic boundary condition. The state of one site i, at a given time t, is denoted by $Z_i(t)$, where $Z_i(t) \in S, E, I, R$ if the individual in the site is susceptible, exposed, infected or recovered, respectively. The state sets are defined by the following sets:

$$\begin{aligned} S &= \{0\}, \\ E &= \{1, \ldots, t_e\}, \\ I &= \{t_e + 1, \ldots, t_e + t_i\}, \\ R &= \{-1\}, \end{aligned} \tag{2}$$

where t_e and t_i are the latency and the infection time of the disease, respectively.

Each site can interact with the closest four neighbors. As we stated before, the state of an individual changes in a sequencing way ($S \to E \to I \to R$). In this way, the site state also changes in the same way, according to a set of transition rules defined below.

2.1.1. Transition $S \to E$

One susceptible individual becomes exposed with a probability P defined by [8],

$$P = \frac{n_e P_e + n_i P_i}{4}, \tag{3}$$

where n_e and n_i indicate the number of exposed and infected individuals in the neighborhood of the site i ($Z_i = 0$). P_e and P_i are probabilities related to the disease, where P_e is the probability in which one exposed individual transmits the infection and P_i is the probability of an infected individual to infect a susceptible one. In this study, we follow the model in equation (1), hence, we set $P_e = 0.0$ and as a result the exposed individuals do not contribute to the infection of susceptible ones. Therefore, a susceptible individual becomes exposed with a probability $P = \frac{n_i P_i}{4}$.

Once the simulations are probabilistic, we select a random number rnd, with $rnd \in [0, 1]$. If $rnd < P$, the transition $S \to E$ occurs to the susceptible site: in a generation $g = t$ the individual is susceptible and in the next generation ($g = t + 1$) the individual becomes exposed. A generation is our time step where all the sites in the lattice are evolved. This process is illustrated in Fig. 1 (a).

2.1.2. Transition $E \to I$

One exposed individual remains in the exposed state until the latent time (t_e) occurs. Consider that in time t the individual became exposed, we have the following

$$Z_i(t) \in E \to Z_i(t+1) = Z_i(t) + 1, Z_i(t + t_e) \in I, \tag{4}$$

where E and I are the sets of states defined by Equation (2).

2.1.3. Transition $I \to R$

One infected individual recovers from the disease with a probability P_{IR}, defined by $P_{IR} = 1/t_i$, where t_i is the infection period. Therefore, the transition $I \to R$ is represented by

$$Z_i(t) \in I \xrightarrow{P_{IR}} Z_i(t+1) = -1, Z_i(t+1) \in R. \tag{5}$$

2.1.4. Mobility and the inclusion of empty sites

One of the main objectives is to study the impact of individual actions on the spread of the disease. In this way, we include the mobility on the grid on our CA model, once one of the impacts of human mobility is a faster disease spread [14]. The movement of individuals is included in a CA model to study different aspects, as the patterns assumed by the individuals in the grid [36,37], the possibility of biodiversity in a cyclic competition model [38,39], the impact of mobility in the spread of infectious disease by vectors [14] and by contact with infected individuals [6,13,16,34].

To include the movement of individuals in our model, we follow the mobility strategy used by Boccara and Cheong in their work about automata network for the SIR model [34]. In this way, we impose the movement to the exchange of places between an individual and an empty site. The mobility occurs randomly: a site is randomly chosen as well as a neighbor; if the site is active (occupied by an individual in any state) and the neighbor is an empty site, the mobility occurs, otherwise, the sites remain unchanged. With the inclusion of the mobility rule, we have two rules: the movement and the state transition of every site. These two rules are applied sequentially, first we consider the mobility and after the mobility rule is applied to every individual, we applied the transition state rule. The mobility process is shown in Fig. 1 (b).

With the inclusion of empty sites, we add a new set of states in equations (2): $Emp = \{-2\}$. Following the inclusion of empty sites, we alter the studied neighborhood of a susceptible individual in

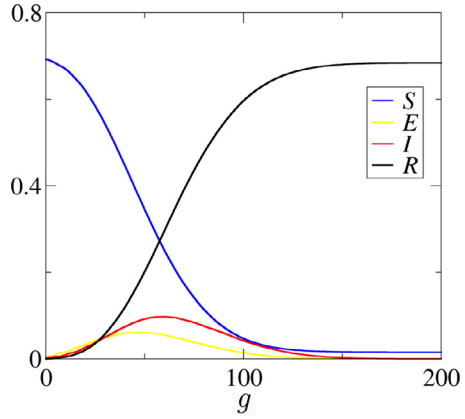

Fig. 2. Time evolution for each population in the SEIR model. In each generation, all the sites are chosen randomly and according to their state, the individual in the site follow the transition rules ($S \to E, E \to R$ and $I \to R$). The blue, yellow, red and black colors indicate the susceptible, exposed, infected and recovered individuals in the grid. The result is an average of 30 simulations. (For interpretation of the references to colour in this figure legend, the reader is referred to the web version of this article.)

the transition $S \to E$: when an empty site is in the neighborhood we consider the next site to enter in the computation of the probability of the infection P. A schematic illustration of the situation is present in Fig. 1 (c).

2.1.5. Initial condition

Now that the transitions rules are defined, we need to specify the initial condition for the CA. We establish that a number N_E and N_I of the sites will contain exposed and infected individuals, on the initial grid. To construct this grid, we randomly chose N_E (N_I) sites and select, also randomly, one value that belongs to E (I). After this step, we randomly choose a fraction f_{emp} of the sites to be empty $Z_i(t=0) = -2$, to enable mobility. The rest of the sites are set to the susceptible state $Z_i(t=0) = 0$.

Evaluating the model described by the last sections (2.1.1 to 2.1.4), we obtain the following time evolution for each population of the SEIR model (Fig. 2) for $P_i = 0.7$, $N_E = 75$, $N_I = 0$, $t_e = 6$, $t_i = 10$, $N = 100$ and $f_{emp} = 0.3$. The values of these parameters are all fixed, except f_{emp}, for all paper. The magnitude of each population is the density related to the total number of sites in the grid. In every generation g, all sites are evolved.

Analyzing the time evolution presented in Fig. 2, we observe the similar form obtained by the differential equation models [22]. The susceptible population decreases as the recovery population increases over time until a stationary value achieved when the disease spread ends. The exposed and the infected populations increase until a maximum value and then they decrease and assume a null value in the end of the epidemics. In this way, our model can be considered to reproduce the behavior of the SEIR model. We perform some tests for greater values of N and observe that if the proportion N_e/N^2 is the same for all values of N, the results are similar. Keeping this proportion, the peak value of the curve I and the generation g when the peak occurs are practically the same. To be more precise, the difference is less than 0.0006 for the peak of I and less than 2 generations of difference for when the peak occurs.

2.2. Infection control and relaxation of control measures

We propose the infection control by individual mobility restriction on the grid and by the decrease of the infection probability P. By this framework, we consider the transformation of some empty sites in "blocked sites", which are sites that do not participate in the mobility and protect the susceptible neighbors.

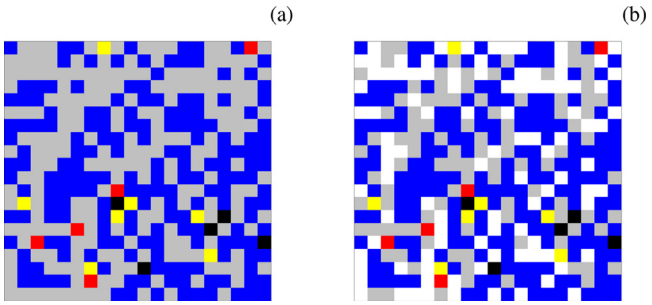

Fig. 3. Lattice (a) before and (b) after the implementation of control in the lattice. The schematic lattice is of size 20×20. The blue, yellow, red and black sites represent susceptible, exposed, infected and recovered individual. The gray sites are empty sites and the white sites, only present in the lattice in (b), are the "blocked sites". In this figure, $N = 20$, $f_{emp} = 0.5$ and $q = 0.5$. (For interpretation of the references to colour in this figure legend, the reader is referred to the web version of this article.)

The proposed control method for our CA model is the transformation of a fraction q of empty sites in blocked sites, when the amplitude of the infected population reaches a value $I_{\max}$. In Fig. 3, we show the implementation of the control in a schematic lattice.

The inclusion of blocked sites decreases the number of individuals moving on the lattice and, consequently, decreases the probability of an infected individual reaching a susceptible one and spreading the disease. The blocked sites also decrease the infection probability P: when they are in the neighborhood of a susceptible individual they act as a shield, once the action of the infected individual right next to the blocked site is neutralized.

After the implementation of the control, we simulate the easing of control measures and modify the scenario to a case with fewer blocked sites. In this study, we consider the relaxation of control in order to analyze the possibility of a second wave of infection in the model. We propose the relaxation when the amplitude of the infected population reaches a minimum value $I_{\min}$, after the first peak of the disease spread, and the relaxation occurs by the return of all the blocked sites to the empty site state. With this relaxation, the mobility and the infection probability recover their pre-control state, as shown in Fig. 3, the panel (b) returns to the scenario in Fig. 3 (a).

In the next section, we present our numerical simulations about the control and the relaxation on the model. First, we analyze the impact of different control parameter q in the peak of the infected population. In a second moment, we investigate the possibility of a second wave due to the relaxation of control measures.

3. Numerical results

In this section, we present the results related to the control implementation and to the relaxation of control measures. We set as the limit value for the implementation of control $I_{\max} = 0.008$ and use the same value for the $I_{\min}$, the relaxation of control measures. From our simulations for $q = 1.0$ and $f_{emp} = 0.3$, we observe that the peak of infections (maximum value of I) for $0.001 < I_{\max} < 0.004$ are smaller. The peaks for $I_{\max} = 0.005$ and $I_{\max} = 0.006$ are greater comparing to the peaks of the curves for $0.007 < I_{\max} < 0.01$, which indicates an intermediate behavior. From these observations, we choose an intermediate scenario, $I_{\max} = 0.008$ and emphasize that the choose of $I_{\max}$ can impact in the epidemic scenario, such as the maximum of the infection and, probably, in the second wave scenario. However, in this paper, we do not study the influence of $I_{\max}$. For the next results, we choose two values for

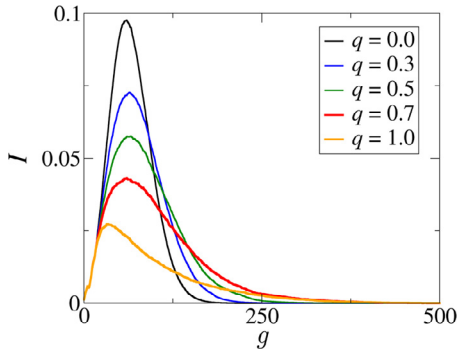

Fig. 4. Control effect on the normalized infected population for different values of control parameter q. All the infected curves are an average of 30 simulations.

$f_{emp} = 0.3$ and $f_{emp} = 0.5$, corresponding to different quantities of empty sites and, consequently, to different mobility scenarios.

3.1. Infection control

For the implementation of control measures, we select a fraction q of empty sites to become barriers, blocked sites. In order to demonstrate the impact of different control magnitudes, we simulate the epidemic for five different values of q: $q = 0.0$ (no control), $q = 0.3$ (low control), $q = 0.5$ (medium control), $q = 0.7$ (high control) and $q = 1.0$ (maximum control). The time evolution of the density of infected individual for all these different control magnitudes are shown in Fig. 4.

For the curves in Fig. 4, we can conclude that an increase of the control parameter q decreases the peak amplitude of the infected curve and extends the duration of the disease spread. The control method that we propose in this model presents the expected result for control measures in an epidemic spread model, namely the peak amplitude decreases more for higher control and the duration of the spread is longer. As the peak amplitude decreases, the total number of infected at the same time is lower, which is beneficial for the health system to avoid its saturation.

A similar result was showed by Lima and Atman (Ref[13].) with their model based on a combination of an agent-based model with probabilistic cellular automata. The paper proposed the inclusion of two methods to control the disease spread, first with the restriction to mobility and, secondly, with the consideration of mask used by individuals. The model proposed by Lima and Atman is more complex and considered more elements, like the heterogeneity of the population and the use of personal protective equipment. Comparing our results on the impact of mobility restriction with those presented in Ref[13]., in both surveys, we observe that stronger restrictions lead to a decrease in the peak of the infected curve and the impact is more effective for restrictions near to lockdown, in which the mobility is almost null ($q > 0.7$ in our case and restriction greater than 70% in their results). However, the decreased peak of the infect curve happens in a different way for both researches. In our model, the peak, for the restricted case, happens almost in the same generation as the peak for the non-controlled case, as we observe in Fig. 4 for $q = 0.3$, $q = 0.5$ and $q = 0.7$. For the Lima and Atman model, the occurrence of the decreased peak is delayed and occurs some time later, when compared to the unrestricted case. These differences must be a consequence of different control methods in the models. For our case, the restriction occurs after the infected curve reaches a certain value, while for the Lima and Atman model the restriction is present all the time.

In Table 1, we present the total number of sick individuals for each curve shown in Fig. 4. From the results in Table 1, we observe that for higher values of the control parameter q the total number of infected individuals is lower, but by the observation of Fig. 4, the duration of the spread is longer. In this way, we can conclude that the implementation of the control is important due to a lower number of infected individuals and the decrease in the number of possible deaths from the disease. In order to enlighten the decrease, we also present in Table 1 the percentage difference related to the total number of infected individuals for the case without control ($q = 0.0$).

Table 1
Total number of infections and relative percentage difference, related to the case with no control, for different values of control parameter q.

Control parameter q	Total number of infected individuals	Relative percentage difference
0.0	68,577	-
0.3	66,256	3.4 %
0.5	63,470	7.4 %
0.7	56,793	17.2 %
1.0	32,006	53.3 %

In Table 1, we verify a decrease of the total number of infected individuals with the implementation of control measures. For lower values of q, the decrease is lower than 10% while for $q = 0.7$, the decrease is 17%. For the total control case, the decrease is higher than 50%. With this result, we can conclude that it is necessary to implement a control with $q > 0.7$ to obtain a reduction greater than 15% in the number of cases.

In the next section, we will study the consequences of easing control. With the analysis of a possible second wave, we observe the impacts of the disease spread in the grid in a more "realistic" scenario, once it is impossible to maintain the control measures during a long time due to economic reasons.

3.2. Relaxation of control measures

For the relaxation of control measures in our model, we follow the steps defined in Section 2.2. The time evolution of the lattice occurs without control until the value of I reaches $I = I_{\max} = 0.008$ and a fraction q of the empty sites becomes "blocked" sites. After the peak of the disease spread (maximum value of I), the curve I decreases and, when the value of I reaches $I = I_{\min}$, the relaxation occurs and all the blocked sites turn into empty sites again (equivalent to $q = 0.0$ situation). In this study, we choose $I_{\min} = 0.008$, *i.e.*, when the epidemic state returns to the situation in which control was implemented.

In order to study different scenarios of control and its subsequent relaxation, we simulate the evolution of the epidemic, for the CA model with control and relaxation, for different values of q and we choose $g = 500$ generations as the length of time series. The result is shown in Fig. 5.

In Fig. 5, we show several time series for the infected population for different values of q. The magnitude of the I curve is represented by the color scale. For both cases, $f_{emp} = 0.3$ (Fig. 5 (a)) and $f_{emp} = 0.5$ (Fig. 5 (b)), the higher values of I are concentrated in the beginning of the evolution ($g \lessapprox 100$) and for lower values of q. From this observation, we can conclude that for less control ($q < 0.4$) the infected curve presents a higher peak and, after it, the spread ends for $g \approx 200$, namely the density of infected individuals is higher but the infection ends sooner, even with the relaxation of control measures.

When a higher control is applied in the system ($q > 0.4$), we see an extension of the blue region, in Fig. 5 (a) and (b), with light blue regions separated by a dark blue section. Following the color scale, this scenario represents two peaks separated by a section of lowers values of I, which characterizes a scenario of a second wave of infections [22]. To elucidate this scenario, we plot some curves

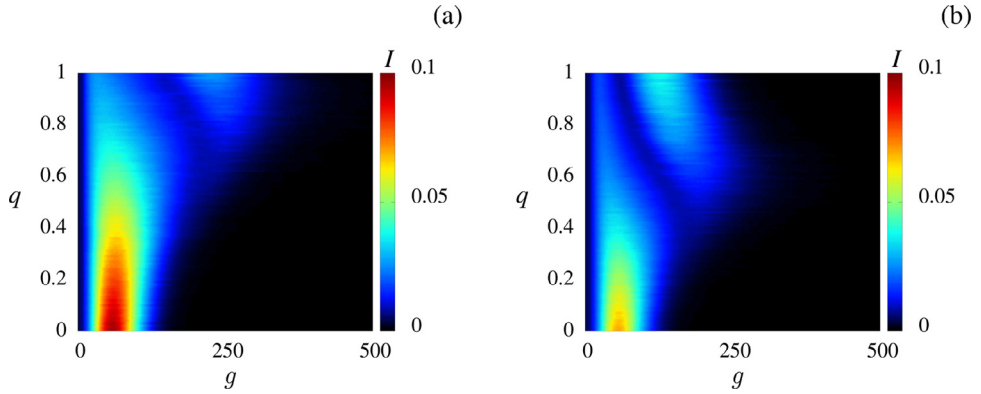

Fig. 5. Time evolution for the density of the infected population for different values of the control parameter q. The relaxation occurs when $I = 0.008$ after the peak of the infected curve I. (a) $f_{emp} = 0.3$ and (b) $f_{emp} = 0.5$. All time evolutions are an average of 30 simulations.

of I for four values of q: $q = 0.0$ (no control), $q = 0.4$ (apparently no second wave), $q = 0.8$ and $q = 1.0$ for high and total control, respectively. The time evolutions for I are shown in Fig. 6 (a) and (c). We also present, in Fig. 6, the total value of infected individuals, I_T, for the same control parameter q and for $f_{emp} = 0.3$ (Fig. 6 (b)) and $f_{emp} = 0.5$ (Fig. 6 (d)).

From the curves shown in Fig. 6 (a) and (c), we observe a second peak in the curve, for $q = 0.8$ and $q = 1.0$, indicating a second wave scenario in the model. For a lower value of q, $q = 0.4$, a second peak is not present but we see a change in the decay in the end of the disease spread. When the relaxation occurs in $q = 0.4$, the decay slope increases, leading to a slower decay, but the mitigation of the control measure is not enough to initiate a second wave of infections. This outcome is explained by the shortage of susceptible individuals after the first wave of infection. The scenario is different for $q = 0.8$ and $q = 1.0$, in which the amplitude of the first peak is comparatively smaller and the decay of the infection curve occurs long before the curves for $q = 0.0$ and $q = 0.4$. In this way, there is a larger number of susceptible individuals available to the infection what causes the second peak when the control measures disappear.

It is important to state that the lower values of I and I_T for the Fig. 6 (c) and (d), in comparison to the curves in Fig. 6 (a) and (b), are a consequence of the different values of empty sites. Once the density I is related to the total number of sites, the highest value of I for the case $f_{emp} = 0.5$ is lower than for $f_{emp} = 0.3$, due to the lower number of active sites.

Observing the total number of cases in Fig. 6 (b) and (d), the cases with relaxation present a cumulative number lower than for the case with no control during all the simulations. For $f_{emp} = 0.3$, the cases for $q = 0.4$ and $q = 0.8$ follow the rule that intense control measures decrease the total number of infections. The exception occurs for $q = 1.0$, where the total number of infection surpasses the number for $q = 0.8$. Now, for $f_{emp} = 0.5$, we verify a different scenario. For higher values of q, $q = 0.8$ and $q = 1.0$, the total number of infections is higher than for the case of lower value of q, $q = 0.4$. However, for all the cases with control, the cumulative number of infections is still smaller than for the case without control.

We conclude that the relaxation can generate a second wave of infections and the total number of cases may be close to the case with no control. Thus, the implementation of control measures and the choice to relaxing these measures have a great impact in the disease spread and in the total effect of the disease in the lattice.

In order to demonstrate how the waves of infection occur in the lattice, we plot the grid for the local maximums and minimums of the infected curve for the case in orange in Fig. 6 (a), i.e., $q = 1.0$ and $f_{emp} = 0.3$. The grids are shown in Fig. 7.

As we observe in Fig. 7, the infection occurs at some different places distributed in the lattice, as we observe several red sites in the grid. This occurs due to the fact that we consider $N_E = 75$ exposed individuals at the initial generation. The peaks occurs at $g = 29$ (Fig. 7 (a)) and at $g = 204$ (Fig. 7 (c)). They are represented by a higher concentration of red sites in the lattice. The waves of infections happen in a distributed way in the lattice, in which the emergence of infected individuals occurs in different parts of the space. We point out that the first wave occurs during the control moment, all the empty sites are blocked (white sites) and no mobility is possible. The minimum of the infected curve is represented in Fig. 7 (b), a snapshot at $g = 130$. As we observe, the number of red sites is lower and the majority of the grid is composed of blue and gray sites. In Fig. 7 (d), we see the lattice at the end of the spread, in which there are no red or yellow sites, only susceptible and recovered individuals and empty sites. With this result, we can understand how the waves of infection occur in the lattice, they occur in different places in the grid due to mobility and the to various exposed individuals in the initial condition.

4. SEIRS Model - inclusion of reinfection

In this section, we consider a temporary immunity of the individuals, *i.e.*, the recovered individuals can become susceptible again. When the reinfection is considered, as the SEIRS model, we need a new transition rule, give by $R \to S$. For our model, we propose and study two different transition rules: fixed immunity time and probabilistic.

4.1. Transition rule $R \to S$: Fixed immunity time

Similarly to the transition $E \to I$ described in equation (4) from Section 2.1.2, we propose the transition $R \to S$ as,

$$Z_i(t) \in R \to Z_i(t+1) = Z_i(t), Z_i(t + t_{imm}) \in S. \tag{6}$$

From this rule, a individual stays in the recovered state for a time t_{imm}, and then becomes susceptible.

In order to study the impact of the immunity loss of the individuals in the lattice, we include the rule from equation (6) in our model with the implementation and relaxation of control measures. For a case with control and immunity loss, we study different combinations of the control parameter q and the immunity time t_{imm}.

We analyze the possibility of the extinction of the epidemic with the chance of reinfection, by the implementation and relaxation of control measures. Thus, we study the averages of the infection peaks for different values of q and t_{imm}. For this computation, we evolve the lattice, for the same parameters values used in

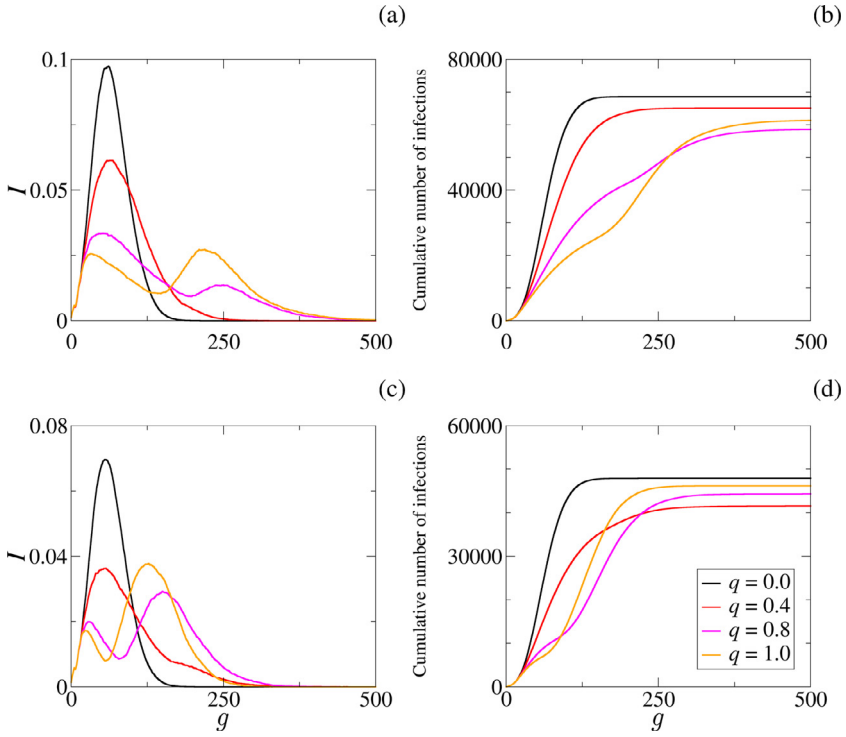

Fig. 6. Time evolution for the density of the infected population for some values of the control parameter q for (a) $f_{emp} = 0.3$ and (c) $f_{emp} = 0.5$. The accumulated value of infected individuals are present in the right column: (b) $f_{emp} = 0.3$ and (d) $f_{emp} = 0.5$.

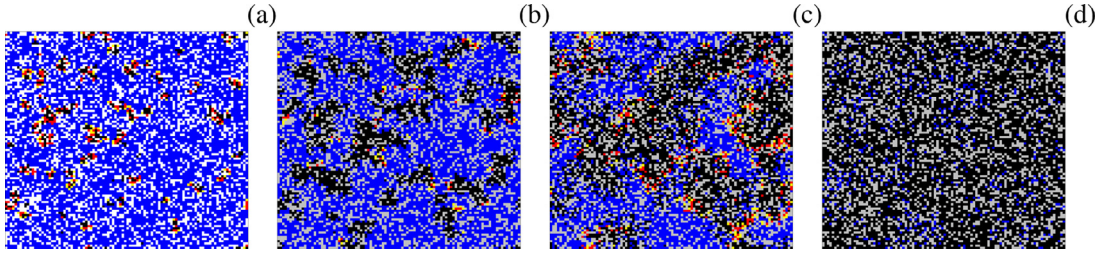

Fig. 7. Grids for different scenarios of infection for $q = 1.0$ and $f_{emp} = 0.3$, the orange curve in Fig. 6 (a). The grids in (a) and (c) are respective to the peaks of the curve, at generations $g = 29$ and $g = 204$, respectively. In (b), we have the snapshot of the lattice for $g = 130$, relative to the valley between the two peaks. At last, (d) represent the system at $g = 500$, the end of the disease spread.

Fig. 5, for 1000 generations and then, for the last 500 generations, we compute the average of the local maximums of the curve I. We calculate this average I_{av} for different values of q and t_{imm}. The results are presented in Fig. 8 for $f_{emp} = 0.3$ and $f_{emp} = 0.5$. The implementation and relaxation of control measures are applied in the same according to Figs. 5 and 6. As we established for the other results, we calculate for an average of 30 simulations.

In Fig. 8, the color scale indicates the magnitude of I_{av}. The colored regions display combinations of q and t_{imm} for which the epidemic does not end in 1000 generations. Meanwhile, for the black region, we observe situations related to the extinction of the epidemic, even with the relaxation of control measures and the reinfection. The higher values of I_{av} are more present for lower values of t_{imm}. As we see, even for a total control measure $q = 1.0$, the average is high: $I_{av} \approx 0.05$ for $f_{emp} = 0.3$ and $I_{av} \approx 0.03$ for $f_{emp} = 0.5$. As the value of t_{imm} increases, the average I_{av} decreases for all values of q and for both values of f_{emp}.

From the perspective of the epidemic annihilation, the end of the spread occurs to high values of t_{imm}, $t_{imm} > 210$, and low values of q for both values of f_{emp}. For $f_{emp} = 0.5$, we can also observe annihilation cases for higher values of q and t_{imm}, indicated by the black region in the upper right corner in Fig. 8(b). The first black region, for higher values of t_{imm} and lower values of q can be explained by the fact that, with low control measures (lower values of q), a higher number of individuals are infected in the beginning of the spread, then, when the individuals become susceptible again, there are not more infected individuals to perpetuate the disease spread in the lattice. The second black region for $f_{emp} = 0.5$ is a consequence of a higher control. There are more empty sites and less active individuals so, with $q \approx 1.0$ and $t_{imm} > 360$, the disease can be extinct.

4.2. Transition rule $R \to S$: Probability P_{RS}

For the second type of the transition rule $R \to S$, we consider a probabilistic rule, in which the recovered individual returns to the susceptible state with probability P_{RS}. This rule is similar to the recovery rule, related to the transition $I \to R$, in Equation (5). Therefore, the probabilistic transition rule $R \to S$ is defined by Equation (7),

$$Z_i(t) \in R \quad \xrightarrow{P_{RS}} Z_i(t+1) \in S : Z_i(t+1) = 0. \tag{7}$$

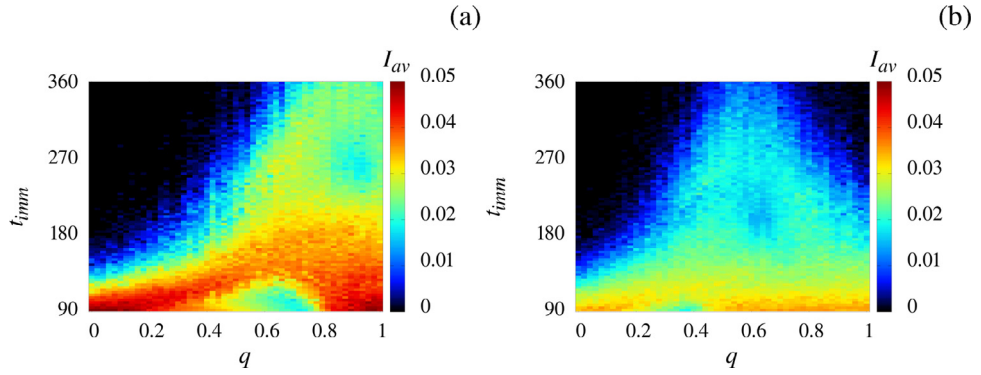

Fig. 8. Parameter space for the SEIRS model, with immunity time fixed, for different values of immunity time t_{imm} and control parameter (q). The color scale indicates the average of the amplitude of I for the last 500 iterations from a time series of length 1000 iterations. The fraction of empty sites in the lattice is (a) $f_{emp} = 0.3$ and (b) $f_{emp} = 0.5$.

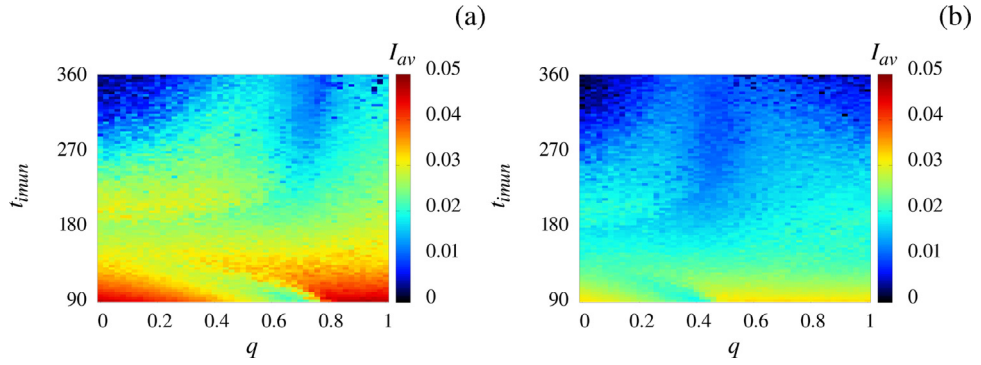

Fig. 9. Parameter space for the average of the amplitude of I (color scale) for the last 500 iterations from a 1000-iterations time series for different values of immunity time (t_{imm}) and magnitude control (q). The fraction of empty sites is (a) $f_{emp} = 0.3$ and (b) $f_{emp} = 0.5$.

The probability P_{RS} is defined according to the immunity time t_{imm}, which is the time that an individual can remain recovered. Following the same logic used for P_{IR} (equation (5)), we define P_{RS} as $P_{RS} = 1/t_{imm}$.

In order to understand how a probabilistic loss of immunity will impact in the epidemic spread, we repeat Fig. 8, considering the transition rule stated in Equation (7) for an average of 30 simulations, as shown in Fig. 9.

Comparing Fig. 8 and Fig. 9, we observe significant different results. As mentioned in the previous section, the case with a fixed immunity time (Fig. 8) presents pairs of q and t_{imm} where the epidemic can be extinct, represented by the black regions. For the probabilistic scenario, the epidemic is rarely over and the average of the infection curve peaks, for the last 500 generations, is non-null for all the pairs (q, t_{imm}) for both $f_{emp} = 0.3$ and $f_{emp} = 0.5$. In Figs. 9 (a) and (b), we see some dark points in the upper region of the parameter space, which indicate values of I_{av} about zero.

Even with a non-null case for I_{av} in Fig. 9, we verify that for higher values of t_{imm}, the average I_{av} is lower, indicating a smaller number of infected individuals for the last 500 generations. For lower values of t_{imm}, the average is higher and decreases for higher values of the immunity time.

If we compare the results for the two transitions rules for $R \to S$ in Figs. 8 and 9, we also observe that the maximum value of I_{av} for both cases are similar. We conclude that, for the proposed control method, the extinction of the epidemic is only possible for high values of t_{imm} and for the case with a fixed immunity time. If the transition $R \to S$ follows the probability $P_{RS} = 1/t_{imm}$, the extinction is not possible and the control only decreases the average I_{av} for higher values of t_{imm}.

5. Conclusions

In this paper, we studied the SEIR epidemic model by a cellular automata portrait. With the proposed model, we could understand the impact of mobility of individuals on the disease spread. As a novelty, we proposed a method to include mitigation measures, as isolation and quarantine in the population. From our mathematical simulations, we conclude that the implementation of control measures decreases the amplitude of the curve of infected individuals and increases the duration of the pandemic, as expected. We also observe that, for a control with more than 70% of the possible paths blocked (blocked sites), the decrease in the total number of infected individuals is greater than 15%, throughout the epidemic. A similar result was obtained by Lima and Atman for a SIR model based on probabilistic cellular automata [13]. The model proposed by Lima and Atman includes 8 different states for the individuals and the heterogeneity of the population is represented by infections of different severities, such as asymptomatic, symptomatic, need for hospital ward or ICU. Through our model, which is simpler, we observe a similar result for the decrease of the infected curve but the shape is different, once it is not flatted for stronger restrictions, and the peak does not suffer a delay for most values of q. Therefore, we affirm that our model can reproduce the impact of restriction of mobility in the disease spread. Our model does not include data from literature, however, we believe that it can be used to model a specific disease.

We also investigate the possibility of a second wave of infections in our CA based model. Our numerical results showed that a second wave scenario is possible and it happens for greater values of the control parameter q. This happens because, with larger con-

trol, there are more susceptible individuals available to become infected when the control measures are relaxed. With this result, we show that the mitigation of restriction measures when the state of the epidemics is the same in which the control was implemented leads to a second wave scenario. Moreover, the total number of infected individuals can be close to the situation with no control.

Lastly, we study the possibility of epidemic extinction for the SEIRS model with only one implementation and attenuation of control measures. We proposed two transition rules for the return of recovered individuals to the susceptible state: fixed immunity time and probabilistic transition. From the parameter spaces for the average of the amplitudes of the curve I, we were able to identify the end of epidemics ($I_{av} = 0$) only for the transition based on fixed immunity time, for higher values of immunity time $t_{imm} > 180$. We can imply that with a longer immunity time, when the recovered individual becomes susceptible, there are no infected individuals to perpetuate the epidemic. For the probabilistic transition, the epidemic persists for all pairs of control parameter, q, and immunity time, t_{imm} combinations.

This survey presents an epidemic model, based on cellular automata, that can be used to study the impacts on the disease spread of the individuals moving in the space. We showed that for some strategies of control and the attenuation of the control measures, it is possible to extinct the epidemic even with the possibility of reinfection, for a fixed immunity time. We considered a homogeneity population, which all individuals respond to the epidemic equally. In future studies, it will be interesting to include heterogeneity in the population, as well as the possibility of pharmaceutical control measures, such as medicines or vaccines.

Credit Author Statment

All the authors contributed equally to this work.

6. Data availability

The data that support the findings of this study are available from the corresponding author upon request.

Declaration of Competing Interest

The authors declare that they have no known competing financial interests or personal relationships that could have appeared to influence the work reported in this paper.

Acknowledgments

We wish to acknowledge the support from the following Brazilian government agencies: Araucária Foundation, National Council for Scientific and Technological Development (CNPq) (140384/2019-7, 407543/2018-0, 302903/2018-6, 420699/2018-0, 407299/2018-1, 428388/2018-3, 311168/2020-5), Coordination for the Improvement of Higher Education Personnel (CAPES) (88887.485425/2020-00) and Fundação de Amparo à Pesquisa do Estado de São Paulo (FAPESP 2018/03211-6, 2020/04624-2). We would also like to thank 105 Group Science (www.105groupscience.com).

References

[1] Brauer F, Castillo-Chavez C. Mathematical models in population biology and epidemiology, vol 2. Springer; 2012.
[2] Murray JD. Mathematical biology i. an introduction, vol 17. Springer-Verlag New York; 2002.
[3] Tomé T, de Oliveira MJ. Stochastic approach to epidemic spreading. Braz J Phys 2020;50(6):832–43.
[4] White SH, Del Rey AM, Sánchez GR. Modeling epidemics using cellular automata. Appl Math Comput 2007;186(1):193–202.
[5] Sun C, Hsieh Y-H. Global analysis of an SEIR model with varying population size and vaccination. Appl Math Model 2010;34(10):2685–97.
[6] Dai J, Zhai C, Ai J, Ma J, Wang J, Sun W. Modeling the spread of epidemics based on cellular automata. Processes 2021;9(1):55.
[7] del Rey AM, White SH, Sánchez GR. A model based on cellular automata to simulate epidemic diseases. In: Cellular Automata. Berlin, Heidelberg: Springer Berlin Heidelberg; 2006. p. 304–10. ISBN 978-3-540-40932-8.
[8] Quan-Xing L, Zhen J. Cellular automata modelling of SEIRS. Chin Phys 2005;14(7):1370.
[9] Wolfram S. Cellular automata and complexity: collected papers. CRC Press; 2018.
[10] German B, Leonardo L, Leonardo G. Modelling population heterogeneity in epidemics using cellular automata. Proceeding of Association Argentina de Mecanica Computacional Rosario 2011;30:3501–14.
[11] Fuentes M, Kuperman M. Cellular automata and epidemiological models with spatial dependence. Physica A 1999;267(3–4):471–86.
[12] Gang J, Liu S, Li S, Zhao Z. A study of the infectious disease with incubation period model based on cellular automata. Commun Math Biol Neurosci 2015;2015 Article ID.
[13] Lima L, Atman A. Impact of mobility restriction in COVID-19 superspreading events using agent-based model. PLoS ONE 2021;16(3):e0248708.
[14] Ortigoza G, Brauer F, Neri I. Modelling and simulating chikungunya spread with an unstructured triangular cellular automata. Infectious Disease Modelling 2020;5:197–220.
[15] Slimi R, El Yacoubi S, Dumonteil E, Gourbiere S. A cellular automata model for chagas disease. Appl Math Model 2009;33(2):1072–85.
[16] Tiwari I, Sarin P, Parmananda P. Predictive modeling of disease propagation in a mobile, connected community using cellular automata. Chaos: An Interdisciplinary Journal of Nonlinear Science 2020;30(8):081103.
[17] Yakowitz S, Gani J, Hayes R. Cellular automaton modeling of epidemics. Appl Math Comput 1990;40(1):41–54.
[18] Ferguson NM, Cummings DA, Fraser C, Cajka JC, Cooley PC, Burke DS. Strategies for mitigating an influenza pandemic. Nature 2006;442(7101):448–52.
[19] Fredj HB, Chérif F. Novel corona virus disease infection in tunisia: mathematical model and the impact of the quarantine strategy. Chaos, Solitons & Fractals 2020;138:109969.
[20] Hellewell J, Abbott S, Gimma A, Bosse NI, Jarvis CI, Russell TW, Munday JD, Kucharski AJ, Edmunds WJ, Sun F, et al. Feasibility of controlling COVID-19 outbreaks by isolation of cases and contacts. The Lancet Global Health 2020;8(4):e488–96.
[21] Zakary O, Bidah S, Rachik M, Ferjouchia H. Mathematical model to estimate and predict the COVID-19 infections in morocco: optimal control strategy. J Appl Math 2020;2020.
[22] de Souza SLT, Batista AM, Caldas IL, Iarosz KC, Szezech Jr JD. Dynamics of epidemics: impact of easing restrictions and control of infection spread. Chaos, Solitons & Fractals 2021;142:110431.
[23] Yu X, Qi G, Hu J. Analysis of second outbreak of COVID-19 after relaxation of control measures in india. Nonlinear Dyn 2020:1–19.
[24] Nadim SS, Ghosh I, Chattopadhyay J. Short-term predictions and prevention strategies for COVID-19: a model-based study. Appl Math Comput 2021;404:126251.
[25] Huang H, Chen Y, Yan Z. Impacts of social distancing on the spread of infectious diseases with asymptomatic infection: a mathematical model. Appl Math Comput 2021;398:125983.
[26] Xu S, Li Y. Beware of the second wave of COVID-19. The Lancet 2020;395(10233):1321–2.
[27] Renardy M, Eisenberg M, Kirschner D. Predicting the second wave of COVID-19 in washtenaw county, MI. J Theor Biol 2020;507:110461.
[28] Brauer F. Epidemic models in populations of varying size. In: Mathematical approaches to problems in resource management and epidemiology. Springer; 1989. p. 109–23.
[29] Li MY, Graef JR, Wang L, Karsai J. Global dynamics of a SEIR model with varying total population size. Math Biosci 1999;160(2):191–213.
[30] Zhang J, Ma Z. Global dynamics of an SEIR epidemic model with saturating contact rate. Math Biosci 2003;185(1):15–32.
[31] Zhang J, Li J, Ma Z. Global dynamics of an SEIR epidemic model with immigration of different compartments. Acta Mathematica Scientia 2006;26(3):551–67.
[32] Li G, Jin Z. Global stability of a SEIR epidemic model with infectious force in latent, infected and immune period. Chaos, Solitons & Fractals 2005;25(5):1177–84.
[33] Röst G. SEIR Epidemiological model with varying infectivity and infinite delay. Mathematical Biosciences and Engineering 2008;5(2):389–402.
[34] Boccara N, Cheong K. Automata network SIR models for the spread of infectious diseases in populations of moving individuals. J Phys A Math Gen 1992;25(9):2447.
[35] Weisstein E.W.. Cellular automaton. https://mathworldwolfram.com/2002;.
[36] Szolnoki A, Mobilia M, Jiang L-L, Szczesny B, Rucklidge AM, Perc M. Cyclic dominance in evolutionary games: a review. Journal of the Royal Society Interface 2014;11(100):20140735.
[37] Reichenbach T, Mobilia M, Frey E. Self-organization of mobile populations in cyclic competition. J Theor Biol 2008;254(2):368–83.
[38] Reichenbach T, Mobilia M, Frey E. Mobility promotes and jeopardizes biodiversity in rock–paper–scissors games. Nature 2007;448(7157):1046–9.
[39] Bazeia D, Menezes J, De Oliveira B, Ramos J. Hamming distance and mobility behavior in generalized rock-paper-scissors models. Europhys Lett 2017;119(5):58003.